

1 Haplotype-resolved genome and population genomics of the 2 threatened garden dormouse in Europe

5 Paige Byerly^{1,2#*}, Alina von Thaden^{1,2#}, Evgeny Leushkin^{1,3}, Leon Hilgers^{1,3}, Shenglin
6 Liu^{1,3}, Sven Winter^{4,5}, Tilman Schell^{1,3}, Charlotte Gerheim^{1,3}, Alexander Ben
7 Hamadou^{1,3}, Carola Greve^{1,3}, Christian Betz⁶, Hanno J. Bolz⁶, Sven Büchner⁸,
8 Johannes Lang⁸, Holger Meinig⁸, Eva Marie Famira-Parcsetich⁸, Sarah P. Stubbe⁸,
9 Alice Mouton⁹, Sandro Bertolino¹⁰, Goedele Verbeylen¹¹, Thomas Briner¹², Lídia
10 Freixas-Mora¹³, Lorenzo Vinciguerra¹⁴, Sarah A. Mueller¹⁵, Carsten Nowak^{1,2}, and
11 Michael Hiller^{1,3,7*}

12
13
14¹ LOEWE Centre for Translational Biodiversity Genomics, Senckenberganlage 25, 60325
15 Frankfurt, Germany

16² Conservation Genetics Group, Senckenberg Research Institute and Natural History Museum
17 Frankfurt, Clamecystraße 12, 63571 Gelnhausen, Germany

18³ Senckenberg Research Institute, Senckenberganlage 25, 60325 Frankfurt, Germany

19⁴ Senckenberg Biodiversity and Climate Research Centre, Senckenberganlage 25, 60325
20 Frankfurt am Main, Germany

21⁵ Research Institute of Wildlife Ecology, University of Veterinary Medicine Vienna, Savoyenstr. 1,
22 1160 Vienna, Austria

23⁶ Bioscientia Human Genetics, Institute for Medical Diagnostics GmbH, Ingelheim, Germany

24⁷ Institute of Cell Biology and Neuroscience, Faculty of Biosciences, Goethe University Frankfurt,
25 Max-von-Laue-Str. 9, 60438 Frankfurt, Germany

26⁸ Justus-Liebig-University Giessen, Clinic for Birds, Reptiles, Amphibians and Fish, Working
27 Group for Wildlife Research, Frankfurter Strasse 114, 35392 Giessen, Germany

28⁹ Socio-économie, Environnement et Développement (SEED), University of Liege (Arlon Campus
29 Environment), Belgium

30¹⁰ Department of Life Sciences and Systems Biology, University of Turin, 10123 Torino, Italy

31¹¹ Natuurpunt Studie vzw, Mammal Working Group, Michiel Coxiestraat 11, 2800 Mechelen,
32 Belgium

33¹² Naturmuseum Solothurn, Klosterplatz 2, 4500 Solothurn, Switzerland

34¹³ BiBio Research Group, Natural Sciences Museum of Granollers, C/ Francesc Macià 51,
35 08402 Granollers, Catalonia, Spain.

36¹⁴ Naturmuseum St.Gallen, Rorschacher Strasse 263, 9016 St. Gallen, Switzerland

37¹⁵ Division of Evolutionary Biology, Faculty of Biology, LMU Munich, Germany

38
39
40 # contributed equally to the manuscript

41 * To whom correspondence should be addressed: paige.byerly@senckenberg.de,
42 michael.hiller@senckenberg.de

43

44 **Abstract**

45 Genomic resources are important for evaluating genetic diversity and supporting
46 conservation efforts. The garden dormouse (*Eliomys quercinus*) is a small rodent that has
47 experienced one of the most severe modern population declines in Europe. We present
48 a high-quality haplotype-resolved reference genome for the garden dormouse, and
49 combine comprehensive short and long-read transcriptomics datasets with homology-
50 based methods to generate a highly complete gene annotation. Demographic history
51 analysis of the genome revealed a sharp population decline since the last interglacial,
52 indicating that colder climates caused severe population declines prior to anthropogenic
53 influence. Using our genome and genetic data from 100 individuals, largely sampled in a
54 citizen-science project across the contemporary range, we conducted the first population
55 genomic analysis for this species to investigate patterns of connectivity between regions
56 and factors explaining population declines. We found clear evidence for population
57 structure across the species' core Central European range. Notably, our data provide
58 strong evidence that the Alpine population, characterized by strong differentiation likely
59 due to habitat isolation, represents a differentiated evolutionary significant unit (ESU). Our
60 data also show that the predominantly declining Eastern European populations show
61 signs of recent isolation, a pattern consistent with a range expansion from Western to
62 Eastern Europe during the Holocene, leaving relict populations now facing local
63 extinction. Overall, our findings suggest that garden dormouse conservation may be
64 enhanced in Europe through designation of ESUs.

65

66

67 Introduction

68 As genomic sequencing technology advances and costs decrease, high-quality
69 reference genomes are becoming increasingly recognized as an essential resource for
70 conservation genomics (Formenti et al. 2022; Brandies et al. 2019; Theissinger et al.
71 2023; Paez et al. 2022). When aligned to a reference genome assembly, high throughput
72 genomic data can contribute to the understanding of past and contemporary population
73 demographics (Gautier et al. 2016; du Plessis et al. 2023; Luo et al. 2023; Campana et
74 al. 2016), reveal evolutionary patterns such as adaptive differentiation (Szarmach et al.
75 2021; Martchenko and Shafer 2023), and provide information about the current
76 conservation status of wildlife species of conservation concern (Talla et al. 2023; Viluma
77 et al. 2022). While reduced-representation sequencing (RRS) methodologies continue to
78 be the more cost-effective and efficient means of generating genome-wide single
79 nucleotide polymorphism (SNP) datasets for large numbers of samples (Wright et al.
80 2020; Peterson et al. 2012), alignment of RRS reads to a high-quality reference genome
81 improves both the precision of SNP calls and the quantity of SNPs recovered when
82 compared to *de novo* read alignment without a genome assembly (Rochette et al. 2019;
83 Brandies et al. 2019). Reference genomes are also useful for data of closely-related
84 species, with cross-species alignment shown to be highly effective (Takach et al. 2023;
85 DeSaix et al. 2019; Burri et al. 2015; Nieto-Blázquez et al. 2022). Given the value of
86 reference genome assemblies for population and conservation genomic analyses,
87 sequencing of reference genomes for wildlife groups should be a focus of ongoing
88 conservation efforts.

89 Highly informative sources of data such as reference genomes can have particular
90 value for investigating understudied wildlife groups, as genomic data can contribute to
91 baseline knowledge necessary for conservation planning. Within mammals, such
92 foundational knowledge is lacking for many small-bodied mammal taxa such as rodents
93 and insectivores, which have a known deficit of research (Verde Arregoitia 2016;
94 Kennerley et al. 2021) that can be seen even in well-studied regions such as Central
95 Europe (Pérez-España 2017). Indeed, general population trends of small mammals are
96 not well understood in Europe (Lang et al. 2022; Pérez-España 2017; Gippoliti and Amori
97 2007; Bertolino et al. 2015), even though many species appear to be declining (Rammou
98 et al. 2022; Gippoliti and Amori 2007; Lang et al. 2022; Reiners et al. 2014). Population
99 genomic analysis could expand our understanding of population structure and the factors
100 contributing to declines, but with the exception of a few flagship species such as the
101 Eurasian beaver (*Castor fiber*; (Halley et al. 2021) it remains a limited tool in European
102 rodent conservation.

103 The garden dormouse (*Eliomys quercinus*) is a small rodent species that
104 exemplifies the small mammal conservation crisis in Europe. Once distributed across the

105 continent, the garden dormouse is now recognized to have experienced one of the most
106 extensive modern population declines on the European continent, with an approximate
107 51% range contraction since the 1970s (Bertolino 2017). Currently, it is only considered
108 common in five of the 26 countries that once comprised its historical range, and even
109 within these refuge countries its distribution is patchy and highly localized (Bertolino
110 2017). Despite its known imperiled status, research on the garden dormouse has been
111 limited, even in comparison to the three other European species in its family Gliridae
112 (Lang et al. 2022)). In particular, the causes of its population decline are still unclear.
113 Changing climate and intensification of land use have been suggested as possible
114 influences; however, the demographic shift appears to have started prior to major 20th
115 century landscape-level changes (Meinig and Büchner 2012; Bertolino 2017). Despite
116 this possible influence of habitat loss, the garden dormouse also shows signs of being a
117 habitat generalist, and this forest species has also adapted well to urban areas in some
118 parts of its range while essentially vanishing from others (Meinig and Büchner 2012),
119 making its decline an ongoing mystery.

120 Population genetic analysis has been identified as a major research need in
121 garden dormouse conservation (Meinig and Büchner 2012), as genetic data could aid in
122 understanding patterns of connectivity and gene flow between regions and uncover past
123 population processes that may help explain current declines. Prior karyotyping and
124 mitochondrial DNA analyses suggested the existence of four genetically distinct clades
125 within Europe (Perez et al. 2013; Libois et al. 2012), although the existence of hybrid
126 individuals indicated gene flow between clades (Perez et al. 2013). A better
127 understanding of the population structure and genetic diversity within the hypothesized
128 clades could help guide future management priorities and inform both regional and
129 European-wide conservation efforts. Here, we present a high-quality reference genome
130 for the garden dormouse, representing the first such complete genome for both the
131 species and its genus. We then demonstrate the utility of the genome by conducting the
132 first genome-wide analysis of population differentiation across the contemporary range of
133 the garden dormouse.

134
135

136 **Results**

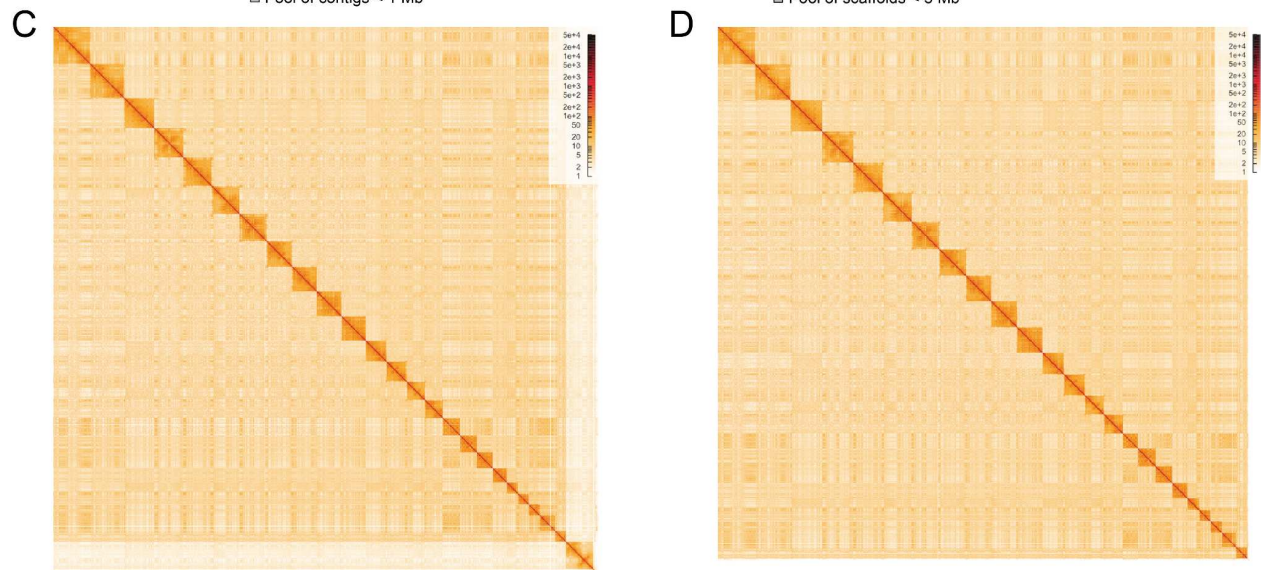
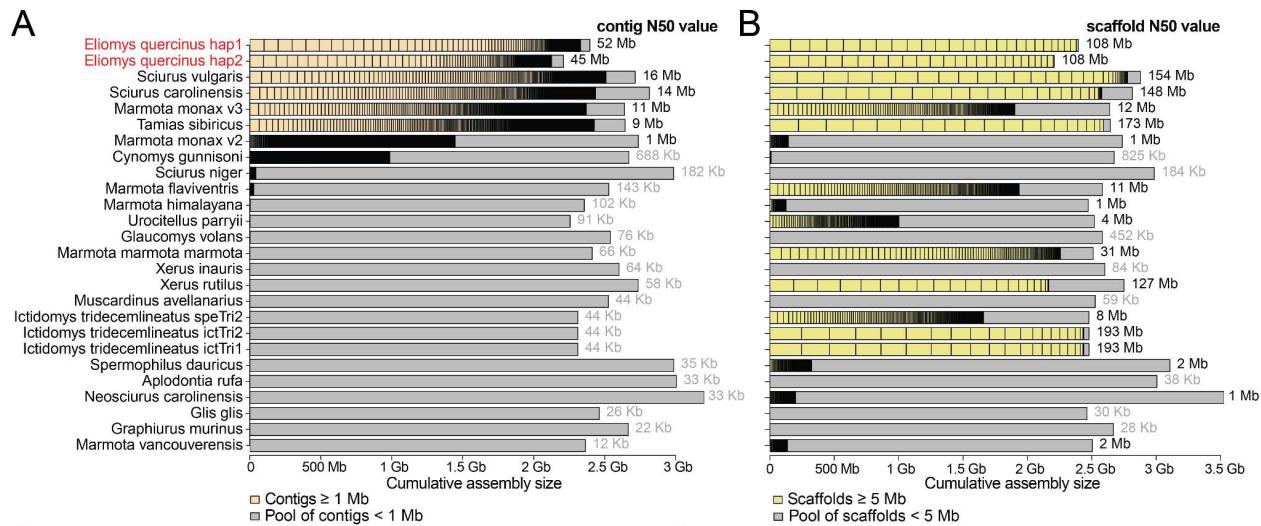
137 **Haplotype-resolved genome assembly**

138 To generate a reference-quality assembly for the garden dormouse, we used long-
139 read sequencing on two PacBio Revio SMRT cells, producing a total of 124.4 Gb of High-
140 Fidelity (HiFi) reads with a HiFi N50 read length of 14 kb. We used the Arima HiC protocol
141 to generate 117 Gbp in long-range read pairs for scaffolding. Assuming a genome size

142 similar to other dormice (Zoonomia Consortium 2020; Böhne et al. 2023) of 2.5 Gb, the
143 HiFi and HiC data have a coverage of ~50X and ~47X, respectively.

144 We used hifiasm (Cheng et al. 2021) in HiC mode to obtain two haplotype-resolved
145 contig assemblies (Fig. S1). The contig N50 values of the two haplotypes are 51.7 and
146 45.4 Mb, respectively. This contiguity is at least 2.8-fold higher compared with other
147 Sciuroomorpha genome assemblies (Fig. 1A,B, Table S1). Scaffold N50 values are 108.1
148 and 107.5 Mb. Haplotype 1 contains the X chromosome, which was assembled as a
149 chromosome-level scaffold. We identified 24 autosomes, inferring that the sequenced
150 individual has a karyotype of 50 chromosomes ($2 \times 24 + 2$ sex chromosomes) (Fig. 1C,D),
151 which matches the range of 48 to 54 chromosomes identified for *Eliomys* so far (Perez et
152 al. 2013). Overall, 99.4 and 99.6% of haplotype 1 and 2 are contained in chromosome-
153 level scaffolds. These metrics exceed the standards set by the Vertebrate Genome
154 Project (Rhie et al. 2021).

155



157 **Figure 1: Contiguity and HiC maps of both haplotype assemblies.**
158 (A, B) Visualization of contig (A) and scaffold (B) sizes of the garden dormouse haplotype 1 and
159 2 (red font) and other Sciuroidea genome assemblies. The N50 values are given on the right
160 side. Contigs shorter than 1 Mb and scaffolds shorter than 5 Mb are not visualized individually,
161 but shown as the grey portion of each bar.
162 (C, D) HiC density maps for haplotype 1 (C) and haplotype 2 (D).

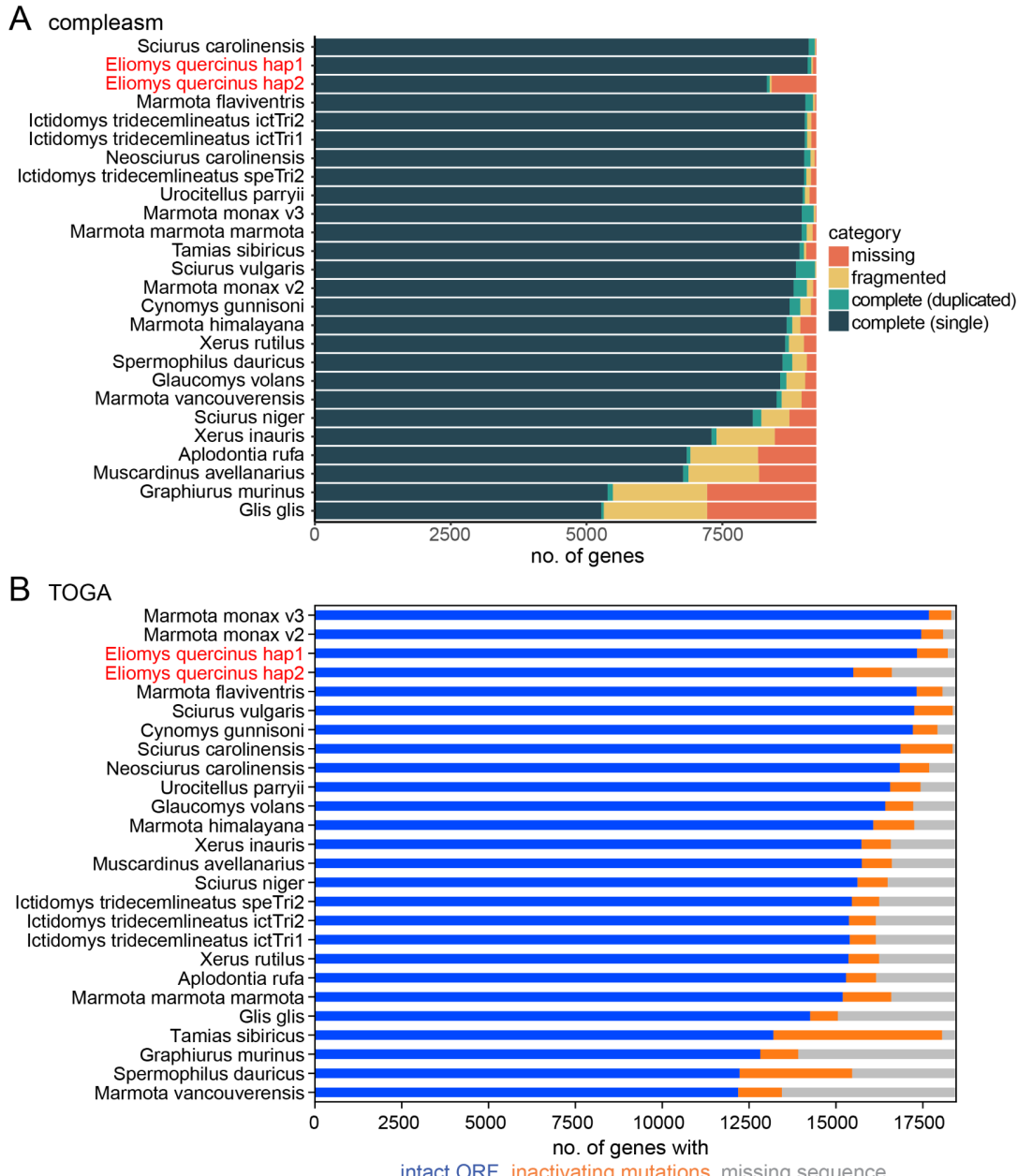
163
164

165 **Assembly quality and completeness**

166 To estimate the assembly base accuracy, we used Merqury (Rhie et al. 2020) with
167 the HiFi reads. Haplotype 1 and 2 have a QV (consensus quality) value of 60.46 and
168 60.24, indicating only one error per megabase. While these QV estimates represent an
169 upper bound as they are based on the HiFi reads used for assembly, these values indicate
170 a very high base accuracy in our assemblies.

171 To assess gene completeness, we first used compleasm 0.2.2 (Huang and Li 2023)
172 with the odb10 set of 9,226 near-universally conserved mammalian genes. Counting
173 completely detected genes present in a single copy, our assemblies contained 98.3%
174 such genes for haplotype 1 and 90.16% for haplotype 2 that lacks the X chromosome. In
175 comparison to other Sciuroidea genome assemblies, our garden dormouse haplotype
176 1 is the second best in terms of this metric after the *Sciurus carolinensis* assembly (Mead
177 et al. 2020) (Fig. 2A, Table S1). Second, we used TOGA (Kirilenko et al. 2023) to compare
178 the status of 18,430 ancestral placental mammal coding genes across the garden
179 dormouse and other Sciuroidea assemblies. TOGA explicitly distinguishes between
180 the two major assembly issues (incompleteness and base errors) by classifying genes
181 into those that have an intact reading frame, those that have gene-inactivating mutations
182 (frameshifts, stop codons, splice site mutations, exon or gene deletions) and those that
183 have missing sequences due to assembly incompleteness or fragmentation. We found
184 that 94.1% of the ancestral genes are intact and only 1.1% have missing exons (Fig. 2B,
185 Table S1). In comparison to other assemblies in the order Sciuroidea, our garden
186 dormouse haplotype 1 is the third best in terms of intact genes. Despite being top-ranked
187 in the compleasm metric, the TOGA analysis reveals that the *S. carolinensis* assembly
188 has substantially more genes with inactivating mutations, indicating a lower base
189 accuracy (Fig. 2B).

190
191



192

193 **Figure 2: Comparison of gene completeness between our haplotype-resolved garden**

194 dormouse and other Sciromorpha genomes.

195 (A) Fractions of detected, fragmented, and missing BUSCO genes (mammalian odb10 dataset,

196 9,226 genes), as classified by compleasm v.0.2.2 (Huang and Li 2023) across Sciromorpha

197 assemblies.

198 (B) TOGA classification of 18,430 ancestral placental mammal genes across Sciromorpha

199 assemblies.

200 Assemblies are ranked by the number of completely-detected (A) and by the number of intact (B)

201 genes. For the garden dormouse, we show both haplotypes in red font and next to each other,

202 but the X chromosome is only contained in haplotype 1. Species and assembly accessions are

203 listed in Table S1.

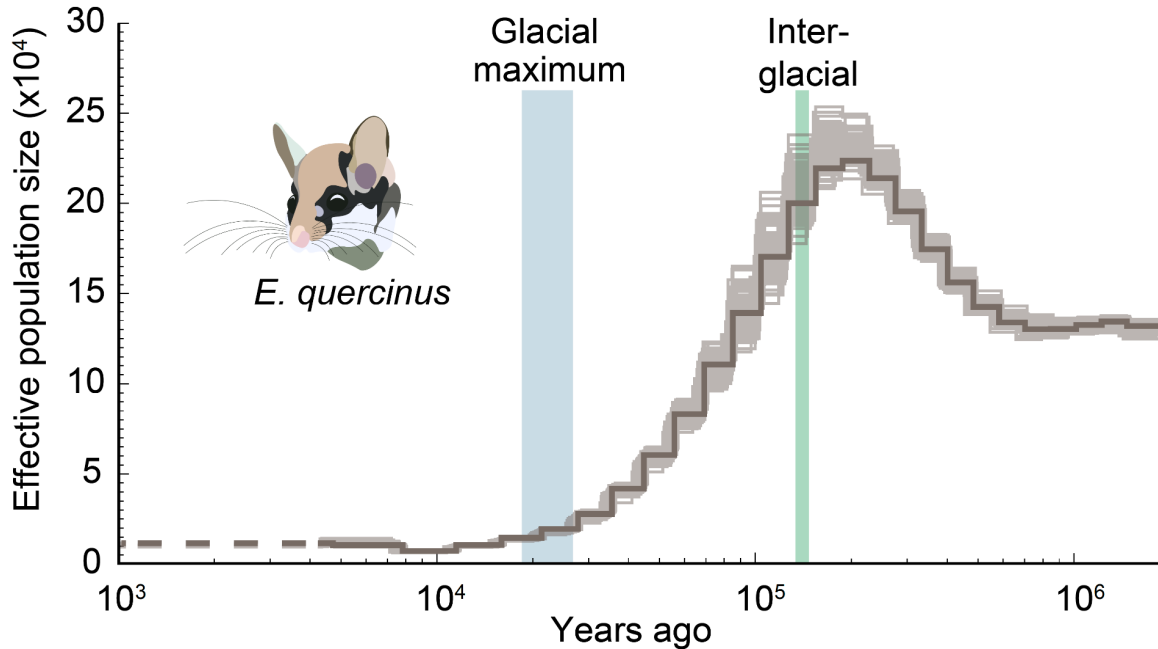
204 **Gene Annotation**

205 To comprehensively annotate genes of the garden dormouse genome, we
206 generated both short-read (RNA-Seq) and long-read (Iso-Seq) transcriptomics data. For
207 RNA-Seq, we sequenced ~4.2 billion reads from eight different organs (heart, testis, liver,
208 lung, spleen, muscle, kidney, and bladder) and for Iso-Seq, we sequenced ~1.6 million
209 reads from six organs (heart, testis, liver, lung, kidney, and bladder) that often cover entire
210 transcripts. The two types of transcriptome data were combined (see Methods) to produce
211 transcript models. In addition to evidence from transcriptomics data, we generated
212 genome alignments and used TOGA (Kirilenko et al. 2023) with the human GENCODE
213 38 and the mouse GENCODE M25 annotation (Frankish et al. 2021) as the reference to
214 provide a homology-based annotation of the garden dormouse. Both types of transcript
215 evidence were joined, which resulted in an annotation comprising 19,374 coding genes.
216 Using compleasm in protein mode, we found that our gene annotation completely
217 contains 99.91% of the mammalian BUSCO genes, indicating a very high completeness.
218

219 **Demographic history of the garden dormouse**

220 To gain insight into the demographic history of the garden dormouse and investigate
221 potential effects of climatic changes in the Pleistocene, we inferred the effective
222 population size (N_e) using pairwise sequentially Markovian coalescence (PSMC) (Li and
223 Durbin 2011). We used a generation time of 1.5 years and a mutation rate of 5.7×10^{-9} per
224 generation (see Methods).

225 Our results indicate relatively high N_e ($> 130,000$) and consistent population growth
226 from 800 kya towards the last interglacial (Fig. 3). Population sizes reached their
227 maximum of $> 200,000$ individuals around the last interglacial. Subsequently, N_e rapidly
228 declined towards the last glacial maximum, reaching an estimated minimum N_e of less
229 than 10,000 individuals around 10 kya. Together, this indicates that the garden dormouse
230 thrived in warm periods, while a cooling climate with longer winters caused severe
231 population declines. Consistent with this result, the Gliridae family thrived during earlier
232 warm periods in the Miocene (23 to 5.3 Mya) (Nadachoswki and Daoud 1995)
233



234

235 **Figure 3: Demographic history of the garden dormouse.**

236 Effective population size (Ne) of *E. quercinus* as estimated with PSMC. Ne in ten thousands is
237 shown on the y-axis and time in years ago on the x-axis. Faint lines indicate uncertainty of inferred
238 Ne based on 100 bootstrap replicates. Blue and green bars show the timing of the last glacial
239 maximum and last interglacial, respectively. The most recent Ne estimate with reduced accuracy
240 is displayed by a dotted line on the left.

241

242

243 **Population genetics**

244 To investigate population structure across the European range of the garden
245 dormouse, we obtained $n = 100$ samples collected opportunistically between 1991–2020
246 for population genomic analyses and performed normalized Genotyping-by-Sequencing
247 (nGBS). After sequencing, reads were aligned to the garden dormouse reference
248 genome, and the resulting alignments were used to call single-nucleotide polymorphisms
249 (SNPs). We assigned *a priori* population identity following in part the clades identified by
250 (Perez et al. 2013) (Fig. 4A).

251 After removal of one individual with 98% missing data and one duplicate sample,
252 we obtained data for a total of 41,175 SNPs from $n = 98$ samples with a mean per site
253 depth of 14.75 X and mean frequency of missingness of 0.11 (Table S2). For analyses
254 dependent upon allele frequencies, such as relatedness and PCA-based analyses, we
255 pruned SNPs based on linkage disequilibrium, resulting in a dataset of 9,131 SNPs.

256 We first inferred relatedness among individual samples using the pruned SNP set
257 and found six pairwise groups of first-order relations in the Harz population. Because

258 inclusion of related individuals can bias population genomic analyses, we randomly
259 removed one individual from each pair above a kinship threshold > 0.35 , which
260 corresponds to a first-order familial relationship, for subsequent analyses (Table S2). All
261 Russian samples were identified as second order relations (kinship > 0.20), indicating
262 half-sibling or grandparent-offspring relationships. Therefore we removed all but one
263 individual from Russia, retaining the sample with the lowest missing data (Table S2). As
264 all individuals with kinship greater than the threshold were collected on the same day from
265 the same locations, these kinship estimates likely reflect accurate estimates of
266 relatedness between individuals. This left us with a final dataset of $n = 86$ samples (Table
267 S2).

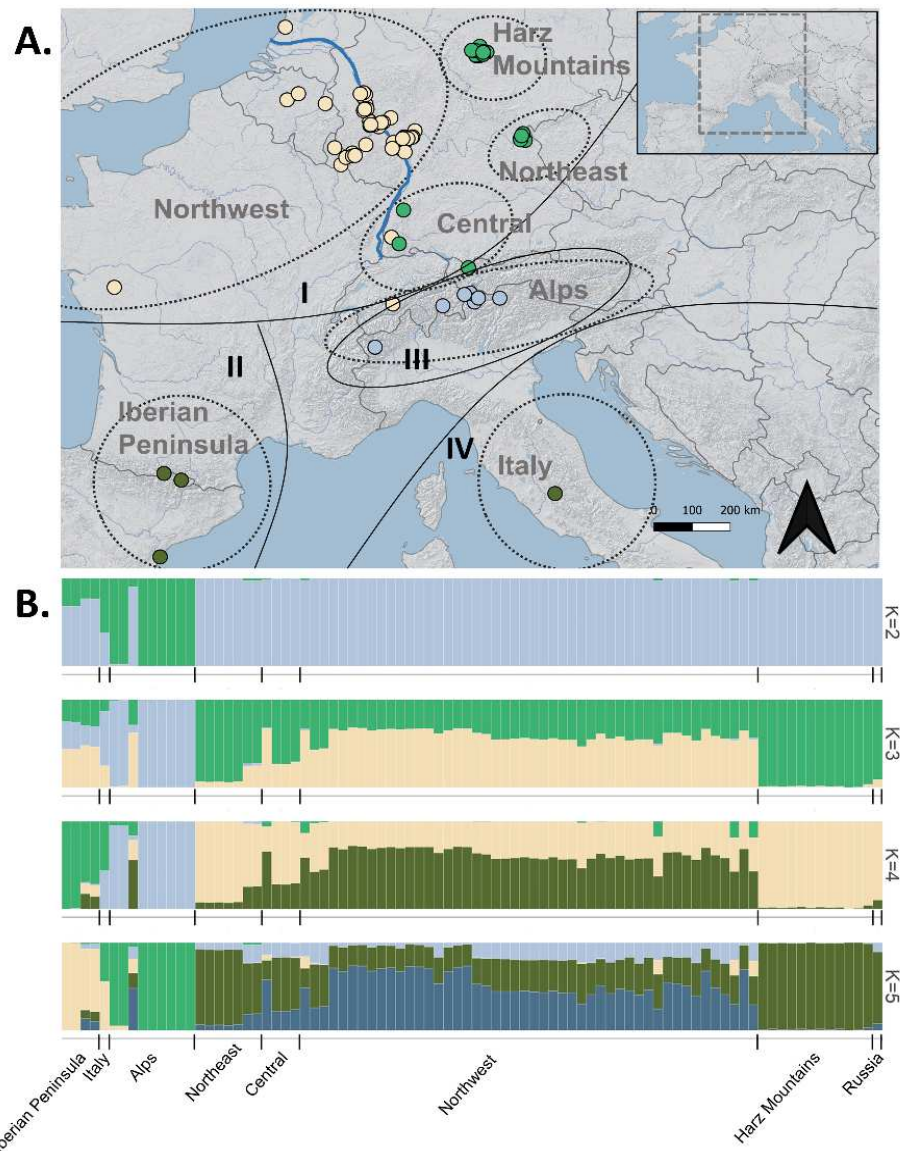
268 Phylogenetic analysis using RAxML showed that individuals from Northeastern
269 Central Europe (Harz Mountains, Central, Northeast, Russia) form a single clade,
270 separated from the Northwest, Alps, Italy, and Iberian Peninsula regions (Fig. S2). This
271 tree conformed with the PCA of genetic distance among individuals and sampling regions.
272 PCA showed a strong separation between the Alpine and other sampling regions, with
273 this differentiation explaining 27.52% of the variation on PC1 (Fig. 5). Further spatial
274 differentiation between the Northwest region and the other Central European sampling
275 locations explained 5.20% of the variation on PC2. These results were consistent with
276 findings of relatively high F_{ST} between most regional pairwise groupings (Table 1),
277 suggesting that dispersal between spatially disjunct populations may be limited.
278
279

	NW	ALP	HAR	CE	IB	NE	IT
ALP	0.54						
HAR	0.15	0.69					
CE	0.08	0.68	0.21				
IB	0.28	0.62	0.44	0.32			
NE	0.13	0.69	0.16	0.11	0.39		
IT	0.43	0.64	0.61	0.53	0.36	0.58	
RUS	0.14	0.79	0.27	0.16	0.40	0.79	0.86

280
281 **Table 1.** Pairwise F_{ST} between eight garden dormouse sampling regions, corrected for sample
282 size. Sampling regions are defined and abbreviated as Northwest (NW), the Alps (ALP), Harz
283 Mountains (HAR), Central (CE), the Iberian Peninsula (IB), Northeast (NE), Italy (IT), and Russia
284 (RUS).

285
286
287 However, the highest overall F_{ST} values were consistently recovered for pairwise
288 comparisons of the Alpine group and all other populations, indicating that differentiation

289 between regions is not only driven by geographic distance, as the Alpine region is
290 relatively central to other sampling sites (Fig. 4A).
291



292
293 **Figure 4. Garden dormouse population structure inferred from 47,115 nuclear SNP loci.**
294 (A) Group assignment via 10 PCs obtained by a discriminant analysis of principal components.
295 (B) The predicted assignment of genetic clusters (K) 1–4 is shown by four different colors, the *a*
296 *priori* sampling region identity is highlighted by dotted gray lines and text. The clades I–IV that
297 were previously identified based on mitochondrial DNA (Perez et al. 2013) are outlined in black.
298 One sample from Russia is not pictured. The Rhine River is outlined in blue, and the boundary of
299 the study area is outlined in grey in the inset map.
300 (B) Genetic clustering inferred by Bayesian structure analysis for K ranging from 2 to 5 in
301 STRUCTURE, with x-axes representing geographic sampling location and y-axes the proportion
302 of group membership.

303 Genetic diversity was highest and inbreeding depression was lowest for the Iberian
304 Peninsula (Table 2). Within the Central European region, genetic diversity was lower for
305 population clusters situated east of the Rhine River (Northeast, Alps, Harz Mountains)
306 compared to those located west of or near the river valley (Northwest, Central). This
307 finding is consistent with the overall lower population sizes of garden dormouse
308 populations located east of the Rhine River in Central Europe (Bertolino 2017), and
309 suggests that eastern populations may be more susceptible to negative effects of recent
310 population declines and range contractions, including isolation and loss of genetic
311 diversity.

312
313

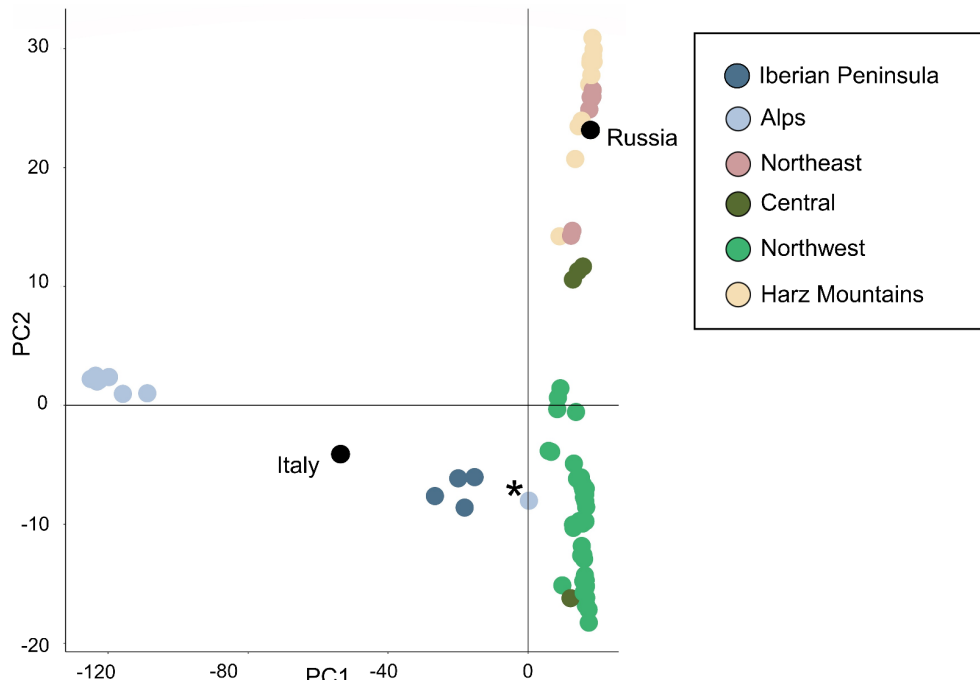
Region	<i>n</i>	A_R	H_{obs}	H_{exp}	F_{IS}
Alps	9	1.11	0.04	0.12	0.62
Central	4	1.20	0.16	0.21	0.15
Harz Mountains	12	1.14	0.13	0.14	0.08
Iberian Peninsula	4	1.24	0.22	0.25	0.06
Italy	1	1.03	0.03	—	—
Northeast	7	1.16	0.13	0.16	0.18
Northwest	48	1.22	0.17	0.22	0.2
Russia	1	1.07	0.07	—	—

314
315 **Table 2.** Sample size (*n*) and genetic diversity metrics among eight garden dormouse
316 sampling regions, with observed (H_{obs}) and expected (H_{exp}) heterozygosity, allelic richness rarified
317 by sample size (A_R), and the inbreeding coefficient F_{IS} .

318
319

320 We used DAPC and STRUCTURE to infer the number of genetic clusters within
321 our samples. Both methods identified $K = 4$ as the most probable number of genetic
322 clusters, although results were clearer for DAPC (Fig. S3A) than for STRUCTURE, which
323 also suggested $K = 2$ and $K = 3$ as possible cluster numbers (Fig. S4). Cluster
324 membership for DAPC was suggestive of relatively strong differentiation between the
325 Northwest region versus other regions in Germany (Fig. 4A, Fig. S3B,C), while
326 STRUCTURE indicated greater admixture among these regions at all values of K (Fig.
327 4B; Fig. S5). Both methods were consistent in differentiating the Alpine samples from all
328 other regions (Fig. 4B; Fig. S5). Patterns observed for the full dataset were comparable
329 for the STRUCTURE analysis subset by sample size (Fig. S6), indicating that our results
330 were not influenced by unequal sample size among our sampling regions for regions
331 where $n > 1$.

332



333

334 **Figure 5. Principal component analysis (PCA) for the garden dormouse.**

335 The PCA is based on 9,130 nuclear SNP loci, with colors representing the geographical origin.
336 Results are plotted on the first two principal components, with PC1 explaining 27.52% and PC2
337 5.20% of variation within the dataset. Regions where $n = 1$ (Italy and Russia) are indicated by
338 black circles, with region names labeled within the plot. One individual from the Alps clustered
339 separately from the Alpine region and is marked with a *.

340

341

342 Overall, population genomic analyses consistently revealed little evidence for
343 contemporary gene flow between the Alpine region and other populations, and the high
344 degree of differentiation in this region may indicate long-term isolation of the Alpine group.
345 Despite the clear isolation of the Alpine group, all analyses were consistent in separating
346 one individual from other samples collected from the Alpine region (G190088CH). This
347 individual, which was collected north of the main Alpine ridge, instead showed strong
348 evidence for admixture with the Northwest and Harz Mountains regions (Fig. 4; Fig. 5).

349

350

351 **Discussion**

352 This study makes a valuable contribution to the conservation of small mammals in
353 Europe by providing a high-quality reference genome for the garden dormouse, the first
354 for its genus. This study was performed in the frame of the citizen-science focused project
355 *Spurensuche Gartenschläfer* ('In Search of the Garden Dormouse'), which is the first

356 over-regional conservation and research project for this species in Germany (Meinig et
357 al. 2023). The project aims at restoring garden dormouse populations, as the species
358 continues to decline across much of its range (Lang et al. 2022). Using this assembly and
359 population genomics data from samples across the species' range, we were able to
360 investigate garden dormouse demographic history, as well as contemporary population
361 structure and genetic diversity parameters.

362 The inferred demographic history indicates that garden dormice underwent a
363 substantial population bottleneck already prior to anthropogenic influence, with rapid
364 decline and long-term low N_e following the last interglacial. Our data suggest that warm
365 periods around the last interglacial period supported high effective population sizes, and
366 that hibernation did not save garden dormouse populations from declining during the last
367 ice age. Previous paleontological data suggested that Gliridae diversified during periods
368 of high glaciation (Lu et al. 2021). This observation has been interpreted as a sign that
369 this family thrived during cold periods, likely because hibernation was an evolutionary
370 advantage to survive cooling climates (Lu et al. 2021). In contrast, our results provide
371 evidence that garden dormouse populations declined by more than 90% as the climate
372 cooled down as it approached the last glacial maximum, raising the possibility that the
373 observed lineage diversification during glaciation might rather have resulted from
374 population fragmentation. This finding is in line with longer winters leading to reduced
375 fitness following later emergence from hibernation (Lane et al. 2012). Similar results of
376 declining populations after the last interglacial period have further been described for
377 other Sciromorphida, including the hibernating Gunnison's Prairie Dog *Cynomys*
378 *gunnisoni* (Tsuchiya et al. 2020) and the Southern Flying Squirrel *Glaucomys volans*
379 (Wolf et al. 2022)

380 Our population genomics analysis found clear evidence for population structure
381 across the species' core Central European range, with strong differentiation in particular
382 for the Alpine region. Our findings of high genetic differentiation and four potential genetic
383 clusters confirm and extend prior genetic research, which also identified four garden
384 dormouse lineages within a similar sampling area based on mitochondrial DNA
385 haplotypes and chromosome number differences (Perez et al. 2013). We found the Alpine
386 region south of the main Alpine ridge to be strongly differentiated from all other sampling
387 regions, as evidenced by both model-based (STRUCTURE), and non-model-based
388 (PCA) approaches. We also found differentiation of regions south of the Alpine range,
389 which supports that this mountain range may act as a barrier to garden dormouse
390 dispersal (Perez et al. 2013). One specimen collected within our Alps boundary showed
391 admixture with more Northern regions, but, as this specimen was collected north of the
392 main Alpine ridge, it is probable that this region is connected to the more northern
393 populations, rather than this individual accurately representing admixture within the highly
394 differentiated Alpine population. In contrast to prior research, with our more

395 comprehensive datasets, we were also able to detect additional moderate population
396 structure within the Central European clade (Fig. 4), showing a clear pattern of
397 differentiation between east and west Central Europe. Given the varying degrees of
398 differences between these regions, it is likely that these patterns of genetic structure have
399 arisen through different forces, with the Alpine population representing a potential
400 evolutionary significant unit (ESU), while structure within Northern Europe may reflect
401 modern population pressures resulting from habitat fragmentations and population
402 isolation.

403 The range contraction of the garden dormouse is known to be centered in the
404 eastern part of its range, with the species becoming more common and populations more
405 contiguous as one moves further west (Bertolino 2017; Meinig and Büchner 2012). Fossil
406 evidence indicates that the garden dormouse originated in the Iberian Peninsula and
407 spread out into Central Europe during the Holocene, which may mean that remaining
408 garden dormice in Eastern Europe represent small, relict populations on the edge of
409 extirpation (Anděra 1986). It is possible, then, that the differentiation of these more
410 eastern populations may therefore reflect genetic drift resulting from isolation of these
411 populations in the 20th century. Support for this possibility is provided by our preliminary
412 findings of lower genetic diversity and greater rates of inbreeding for the more easterly
413 populations in Germany (Harz mountains and Northeast), while the Central population
414 shows evidence of admixture with the larger and more contiguous Northwest population,
415 thereby potentially increasing its genetic diversity through interbreeding. Larger sampling
416 efforts are required to substantiate these findings that are based on rather low sample
417 numbers. A similar east-west pattern of differentiation has also been observed in the
418 garden dormouses' spatially overlapping relative, the hazel dormouse (*Muscardinus*
419 *avellanarius*), which is distributed as two separate lineages or 'partial ESUs', delineated
420 along a similar geographic divide as the garden dormouse (Leyhausen et al. 2022;
421 Mouton et al. 2017). Unlike the hazel dormouse, however, this east-west pattern of
422 differentiation was not reflected by mtDNA in the garden dormouse (Perez et al. 2013),
423 indicating that the division among lineages may be a more recent phenomenon resulting
424 from habitat fragmentation and/or demographic changes such as population declines.

425 In contrast to the Central European regions, the Alpine population shows a strong
426 signal of genetic differentiation, which confirms prior mtDNA genetic distance estimates
427 (Perez et al. 2013). Within the Alpine region, the garden dormouse is found in both
428 subalpine and montane habitats, where it occupies coniferous as well as deciduous forest
429 habitat (Bertolino 2017). The strong genetic differentiation and the highly differentiated
430 habitat may indicate the potential for longer-term genetic separation, possibly arising from
431 adaptation to local habitat conditions or climate. Evidence for the Alpine population as a
432 potential ESU is further provided by the lower rates of genetic diversity and high estimate
433 of inbreeding indicative of reproductive isolation of the population. Perez et al. (2013) also

434 found lower nucleotide diversity for this region, and surmised that this may have resulted
435 from either population bottlenecks or recent population expansion. By contrast, the
436 relatively high genetic diversity and low inbreeding of the Iberian population likely reflect
437 a rather large population size and contiguous breeding range of the species in the warmer
438 Mediterranean regions, where it is still considered relatively common (Bertolino 2017).
439 Given that we only have one sample from the Italian mainland, our data are not sufficient
440 to infer whether the Iberian and Italian populations are differentiated, and further sampling
441 of this region is needed to establish patterns of relatedness of garden dormouse within
442 the Mediterranean.

443 Although the causes of the garden dormouse's east-to-west pattern of range
444 contraction aren't fully understood, landscape level changes driven by land use and
445 climate change have been partially implicated (Bertolino 2017). However, it is unclear
446 what specific role climate might play in this contraction. For the ecologically-similar hazel
447 dormouse, warmer and wetter winters have been found to have a negative effect on adult
448 survivorship, possibly because warmer temperatures cause animals to wake during
449 hibernation, thereby expending energy and causing a reduction in fat reserves (Combe
450 et al. 2023). Garden dormice hibernate in regions of harsh winter, and their life histories
451 appear strongly tied to winter temperatures, as well as the onset and duration of the
452 season (Bennett and Richard 2021; Mahlert et al. 2018). Timing and duration of activity
453 periods and hibernation vary widely based on local climate conditions, with Mediterranean
454 populations hibernating only 1–2 months per year, if at all, while Alpine populations may
455 hibernate for 7 months per year (Bertolino et al. 2001). While populations appear to be
456 limited by extreme cold (Schaub and Vaterlaus-Schlegel 2001; Bertolino et al. 2001),
457 warm weather during hibernation may also cause stressors that could inhibit population
458 growth in regions where dormouse are more adapted to cold, particularly where winter
459 food resources are not available (Giroud et al. 2023). Further investigation of the role of
460 climate in shaping the garden dormouse's population structure via local adaptation may
461 be useful in predicting the future viability of the species with ongoing climate change.

462

463 Conclusion

464 The garden dormouse is currently listed as "Near Threatened" in the IUCN Red
465 List despite compelling evidence that recent range reductions necessitate relisting the
466 species as "Vulnerable" (Bertolino 2017). Our findings provide strong evidence for the
467 designation of the Alpine subpopulation of the garden dormouse as a separate ESU,
468 given that it fulfills the criteria set by (Moritz 1994) of reciprocal mtDNA monophyly (Perez
469 et al. 2013) and significant nuclear DNA divergence. Overall, findings from this study
470 suggest that garden dormouse conservation may be enhanced in Europe through the
471 designation of differentiated populations as ESUs. Further research is needed to

472 determine if these ESUs are experiencing local adaptation to environmental factors such
473 as temperature, and how these potential adaptations may influence future population
474 viability in the face of a changing climate. Our annotated genome will enable comparative
475 analyses and addressing open evolutionary questions of the *Eliomys* species complex,
476 as well as to inform specific conservation planning and management for the garden
477 dormouse in Europe. It is our hope that the findings outlined in this study can help guide
478 the direction of future research for the garden dormouse, while also highlighting the need
479 for further protection within regions of population isolation and/or low genetic diversity.
480
481

482 **Materials and Methods**

483 484 **Sample collection**

485 Tissue samples for nGBS were collected from across the European distribution in
486 the frame of a larger conservation project on *Eliomys quercinus* in Germany. Samples
487 originated from Germany ($n = 66$), other Central European countries ($n = 25$), and Russia
488 ($n = 7$) and were collected between 1991-2020 (see Table S2). All samples were taken
489 opportunistically from dead-found individuals brought to museums or animal shelters,
490 during monitoring, or during citizen-science activities, and all in compliance with
491 respective local and national laws.
492

493 **Genome sequencing**

494 To sequence a high-quality genome, we used a male individual collected in March
495 2023 in Mainz that was euthanized by a veterinarian due to injuries.
496

497 High molecular weight genomic DNA was extracted from heart tissue according to
498 the protocol of (Sambrook and Russell) for the first library and from lung tissue using the
499 PacBio Nanobind Tissue Kit (PacBio, Menlo Park, CA, USA) for the second library. DNA
500 concentration and DNA fragment length were assessed using the Qubit dsDNA BR Assay
501 kit on the Qubit Fluorometer (Thermo Fisher Scientific) and the Genomic DNA Screen
502 Tape on the Agilent 4150 TapeStation system (Agilent Technologies), respectively. A
503 SMRTbell library was prepared for each tissue according to the instructions of the
504 SMRTbell Express Prep Kit v3.0. Total input DNA was approximately 4 μ g per library.
505

506 Quality control of the final libraries was performed on an Agilent Femto Pulse system
507 (Agilent, Waldbronn Germany). Annealing of sequencing primers, binding of sequencing
508 polymerase, and purification of polymerase-bound SMRTbell complexes were performed
509 using the Revio polymerase kit (PacBio, Menlo Park, CA, USA). Loading concentration
for sequencing was 225 pM. Long-read whole-genome sequencing was performed on a
PacBio Revio instrument (PacBio, Menlo Park, CA, USA), 24 h HiFi sequencing, 15 kb

510 median read length, Q30 median read quality. HiFi read BAM files (128 Gb in total) were
511 used for genome assembly.

512 To generate long-range data for scaffolding, we used the Arima High Coverage Hi-
513 C Kit v01 (Arima Genomics) according to the Animal Tissue User Guide for proximity
514 ligation using approximately 110 mg of heart tissue from the same individual. The
515 proximally-ligated DNA was then converted into an Arima High Coverage HiC library
516 according to the protocol of the Swift Biosciences® Accel-NGS® 2S Plus DNA Library
517 Kit. The fragment size distribution and concentration of the Arima High Coverage HiC
518 library was assessed using the TapeStation 4150 (Agilent Technologies) and the Qubit
519 Fluorometer and Qubit dsDNA HS reagents Assay kit (Thermo Fisher Scientific, Waltham,
520 MA), respectively. The library was sequenced on the NovaSeq 6000 platform at
521 Novogene (UK) using a 150 paired-end sequencing strategy, resulting in an output of 180
522 Gb.

523

524 **Transcriptome sequencing**

525 Total RNA was isolated from bladder, heart, kidney, liver, lung, muscle, spleen, and
526 testis from the same individual using TRIzol reagent (Invitrogen) according to the
527 manufacturer's instructions. The quality and concentration of each extraction was
528 assessed using the TapeStation 4150 (Agilent Technologies) and the Qubit Fluorometer
529 with the RNA BR Reagents Assay Kit (Thermo Fisher Scientific, Waltham, MA). The RNA
530 extractions were then sent to Novogene (UK) for Illumina paired-end 150 bp RNA-seq of
531 a cDNA library (insert size: 350 bp) with a respective expected output of 9 Gb.

532 For the preparation of Iso-seq libraries using the SMRTbell Prep Kit 3.0, only RNA
533 extractions with an RNA integrity number (RIN) > 7 were used, as recommended by the
534 manufacturer's protocol. Two libraries were prepared by pooling RNA from kidney, liver,
535 lung or bladder, heart and testis at approximately 90 ng each, with the exception of lung
536 RNA at approximately 60 ng, resulting in two pooled libraries. These two Iso-Seq libraries
537 were then each loaded onto an SMRT cell sequenced in CCS mode using the Sequel
538 System IIe with the Sequel II Binding Kit 3.1 (Pacific Biosciences, Menlo Park, CA) at the
539 Genome Technology Center (RGTC) at Radboudumc (Nijmegen, The Netherlands). The
540 libraries were loaded to an on-plate concentration of 80 pM each by diffusion loading.

541

542 **Genotyping-by-Sequencing**

543 Tissue samples for nGBS were extracted using the DNeasy Blood & Tissue Kit
544 (Qiagen) with slight protocol modifications to increase yield of RNA-free genomic DNA as
545 described in (Leyhausen et al. 2022). Extracts were quantified with fluorometry (Qubit)
546 and spectrophotometry (NanoDrop) and screened for DNA integrity using gel
547 electrophoresis to identify samples of sufficient quality for NGS. Selected samples ($n =$

548 100) with \geq 300 ng of high molecular weight DNA were sent for nGBS at LGC Genomics
549 GmbH (www.biosearchtech.com). Details on enzymatic digestion, library preparation and
550 nGBS protocols can be found in (Leyhausen et al. 2022; Arvidsson et al. 2016).

551

552 **Genome assembly**

553 We produced haplotype-specific assemblies from HiFi reads using hifiasm
554 (v.0.19.5), integrating HiC reads for phasing (Cheng et al. 2021). Both haplotypes were
555 subject to filtering procedure using Foreign Contamination Screen Tool (FCS) (Astashyn
556 et al. 2023). Contamination free assemblies were then polished to remove unambiguous
557 heterozygous sites. Specifically, we mapped HiFi reads back to each assembly with
558 minimap2 v.2.26 (Li 2018), removed duplicates using picard MarkDuplicates tool v.3.1.0
559 (<http://broadinstitute.github.io/picard>), and called variants using DeepVariant v1.5.0
560 (Poplin et al. 2018). We then filtered for sites with genotype 1/1 and a 'PASS' filter value,
561 meaning that all or nearly all reads support an alternative sequence at this position and
562 passed DeepVariants internal filters. Finally, we corrected corresponding nucleotide sites
563 in the assembly using bcftools consensus v.1.13 (Li 2011).

564 To scaffold the polished haplotype assemblies, we first mapped the Arima HiC reads
565 to each of the two assemblies independently using chromap v.0.2.5 (Zhang et al. 2021)
566 and then processed mapped reads with yahs v1.1a (Zhou et al. 2023). Finally, we
567 performed manual curation of the two scaffolded haplotypes jointly analyzing them in
568 PretextView v.0.2.5 (<https://github.com/wtsi-hpaq/PretextView>). To this end, we
569 remapped the HiC reads to both haplotype assemblies concatenated together using again
570 chromap but allowing for multi-mapping reads (-q 0) to avoid discarding information in
571 regions identical between two haplotypes. We also identified telomeric sequences with
572 tidk v.0.2.31 (<https://github.com/tolkit/telomeric-identifier>) and where necessary corrected
573 wrong contigs orientations to have telomeres in the ends of resulting scaffolds. To finalize
574 changes made via manual dual haplotype curation, as recently proposed by the
575 Vertebrate Genome and Darwin Tree of Life Project, we used the rapid curation
576 framework (<https://gitlab.com/wtsi-grit/rapid-curation/-/tree/main>) from the Genome
577 Reference Informatics Team (Howe et al. 2021).

578

579 **Repeat masking and whole-genome alignment**

580 RepeatModeler version 2.0.4 (default parameters) was used to generate a *de novo*
581 repeat library for the garden dormouse assembly. RepeatMasker 4.1.0 (parameters -
582 engine ncbi) was used with the resulting library to soft-mask the genome.

583 We followed our previous workflow to align the human (hg38 assembly) and the
584 mouse (mm10) assembly to both garden dormouse haplotype assemblies (Sharma and

585 Hiller 2017; Blumer et al. 2022). Briefly, we used LASTZ version 1.04.15 with sensitive
586 parameters (K = 2400, L = 3000, Y = 9400, H = 2000, and the LASTZ default scoring
587 matrix) (Harris 2007), axtChain (default parameters except linear-Gap=loose) to compute
588 co-linear alignment chains (Kent et al. 2003), RepeatFiller (default parameters) to capture
589 additional alignments between repetitive regions (Osipova et al. 2019), and chainCleaner
590 (default parameters except minBrokenChainScore = 75,000 and -doPairs) to improve
591 alignment specificity (Suarez et al. 2017).

592

593 **Gene annotation**

594 We used TOGA (Kirilenko et al. 2023) with the alignment chains and the human
595 GENCODE 38 and the mouse GENCODE M25 annotation (Frankish et al. 2021) to
596 annotate coding genes. We ran TOGA for both garden dormouse haplotypes.

597 Raw RNA-seq data were processed with fastP v0.23.4 (Chen 2023; Chen et al.
598 2018) to remove adapters and low quality (< Q15) bases. Processed reads were mapped
599 to a first haplotype assembly with hisat2 v.2.2.1 (Kim et al. 2019). For Iso-Seq reads a
600 circular consensus was generated from the subreads using ccs v.6.4.0
601 (<https://github.com/PacificBiosciences/pbbioconda>). Adapter trimming and base quality
602 filtering was performed with lima v2.2.0
603 (<https://github.com/PacificBiosciences/pbbioconda>). Processed reads were cleaned from
604 polyA tails and polymerase switching artifacts using 'refine' command from the isoseq
605 package v.4.0.0 (<https://github.com/PacificBiosciences/IsoSeq/blob/master/isoseq-clustering.md>) and then clustered together and aligned to generate consensus reads
606 using the 'cluster' command from the isoseq package. Additionally, reads were filtered for
607 alignment artifacts using a custom perl script. To combine transcriptome information from
608 RNA-seq and Iso-seq, we then used a hybrid option (--mix) in stringtie v.2.1.2 (Shumate
609 et al. 2022).

611 To integrate transcriptomics and homology-based transcript evidence, we first
612 merged human and mouse TOGA, keeping only transcripts with an intact reading frame.
613 We then added transcripts classified as partially intact and uncertain loss, but only if they
614 do not overlap intact transcripts. The RNA- and Iso-seq merged transcriptome data was
615 then used to add UTRs to TOGA-annotated coding transcripts with a compatible exon-
616 intron structure. Finally, we added transcriptome data for genomic loci that don't have a
617 TOGA transcript prediction to incorporate lineage-specific and non-coding transcripts into
618 the annotation.

619

620 **Demographic history**

621 We used PSMC (Li and Durbin 2011) to infer the demographic history of the garden
622 dormouse across the past one million years. Minimap2 v.2.26 (Li 2018) was used to map
623 the PacBio HiFi reads to haplotype 1. Heterozygous sites were called with DeepVariant

624 v1.2.0 (Poplin et al. 2018) using the PacBio model. A consensus genome sequence
625 where the heterozygous sites were represented with IUPAC ambiguity codes was
626 generated using bcftools v1.17 (Danecek et al. 2021). The consensus sequence was
627 converted to the input format of PSMC by applying a bin size of 50 bp.

628 For PSMC, we included data from all chromosome-size scaffolds except for the X
629 chromosome (scaffold 4). PSMC was run using the parameter settings *-N25 -t15 -r5 -p*
630 "*4+25*2+4+6*". We also explored including more parameters (*-p "4+45*2+4+6"* and *-p*
631 "*4+65*2+4+6*") as well as splitting the first parameter (e.g., *-p "2+2+25*2+4+6"*). None of
632 these settings changed the general results, so we chose to use the default parameters.
633 Finally, we calibrated PSMC results using a generation time of 1.5 years and a mutation
634 rate of 5.7×10^{-9} per generation. This mutation rate is based on the assumption that garden
635 dormice exhibit a similar mutation rate as mice, for which the rate is well established
636 (Uchimura et al. 2015; Milholland et al. 2017). The mean generation time (1.57 years)
637 was calculated based on a yearly reproductive cycle starting at age one, a maximum age
638 of 5 years, and an average yearly survival rate of 0.38 (Schaub and Vaterlaus-Schlegel
639 2001).

640

641 **Population genomics**

642 The raw GBS data were trimmed using fastp v0.23.4 (Chen et al. 2018) with enabled
643 base correction and low complexity filter to remove sequencing adaptors and polyG
644 stretches at the end of reads. A 4 bp sliding window was employed to detect regions of
645 poor quality (Phred score < 15). We removed reads if they fit into one of the following
646 categories: read length below 36 bp, reads with > 40% low-quality bases, and reads with
647 5 or more undetermined bases (Ns). The trimmed reads were then mapped against
648 haplotype 1 of our assembly using bwa-mem v0.7.17-r1188 (Li 2013). Mate coordinates
649 in the resulting mapping files were filled in, the files were sorted by position, and indexed
650 using samtools v.1.18 (Danecek et al. 2021). Variant calling was performed with the
651 ref_map.pl pipeline for reference aligned reads in stacks v2.65 (Rochette et al. 2019) with
652 additional filtering parameters given for the populations program: minor allele frequency
653 of 5%, a minimum percentage of individuals per population of 80, and writing one random
654 SNP per locus (*-X "populations: -r 0.80 --min-maf 0.05 --write-random-snp"*). Additional
655 variant filtering was performed with VCFtools v0.1.16 (Danecek et al. 2011) to remove
656 indels and only keep biallelic SNPs with a depth per individual between 6 and 50 (flags:
657 '*--remove-indels --min-alleles 2 --max-alleles 2 --min-meanDP 6 --max-meanDP 50 --*
658 *minDP 6 --maxDP 50*'). After filtering, we removed samples with > 75% missing data to
659 generate our final VCF file.

660 Past mitochondrial DNA work has classified four distinct garden dormouse clades
661 within its European range (Iberian, Italian, Western European, and Alpine; (Perez et al.
662 2013). We followed these clade designations in assigning *a priori* population identity but

663 expanded the 'Western European' category by delineating individuals within this clade as
664 Northwest, the Harz Mountains, Northeast, Central, and Russia (Fig. 4A) as aligning to
665 known garden dormouse distribution within this region (Meinig and Büchner 2012).

666 Because linkage disequilibrium (LD) can influence some analyses such as principal
667 components-based analyses (PCAs) and estimating relatedness between individuals
668 (Malomane et al. 2018), we created a pruned SNP set using the 'snpgds' function in the
669 R package SNPRelate (Zheng et al. 2012) using an LD threshold of $r^2 < 0.2$ and a sliding
670 window of 500bp, which was applied to analyses that rely on allele frequencies for
671 population inferences. We hereafter refer to the 'full' and 'pruned' SNP sets.

672 Excessive numbers of related individuals can bias some population genomics
673 analyses ((O'Connell et al. 2019); (Wang 2018)). Because our sample collection was not
674 always random, we anticipated that several individuals within our sample set were related,
675 and therefore estimated pairwise relatedness within sampling regions in the pruned SNP
676 set using the KING-robust method ((Manichaikul et al. 2010)) in SNPRelate. We then
677 removed 1 from each pair with a kinship estimate > 0.35 , which corresponds to a first-
678 order familial relationship (sibling pair, parent-offspring). This sample set was used for all
679 subsequent analyses.

680 We investigated phylogenetic distance among samples and groups using the full
681 SNP set by inferring a phylogeny in RAxML version 8.2.12 ((Stamatakis 2014)) using the
682 ASC-GTRCAT model with Lewis correction for ascertainment bias with 100 bootstrap
683 replicates. We plotted the tree in the R 4.3 (R Core Team 2022) package GGTREE ((Yu
684 et al. 2017)) with a customized script formulated for SNP marker data ((Severn-Ellis et al.
685 2020)).

686 To explore population structure, we used the pruned SNP set to visualize population
687 clustering via PCA and investigated genetic differentiation by calculating pairwise F_{ST}
688 ((Weir and Cockerham 1984)) between sites with correction for sample size, both in
689 SNPRelate. We compared genetic diversity among sampling regions by calculating
690 observed (H_{obs}) and expected (H_{exp}) heterozygosity, allelic richness rarified by sample
691 size (A_R), and the inbreeding coefficient F_{IS} in Hierfstat v 0.5-11 ((Goudet and Goudet
692 2014)).

693 We estimated the most probable number of genetic clusters K within our sample set
694 using the full SNP set. First, we implemented a discriminant analysis of principal
695 components (DAPC) using the 'find.clusters' function in the R package adegenet
696 ((Jombart and Bateman 2008)) to estimate optimal number of K testing K = 1–8. The most
697 probable number of clusters was identified as the one with the lowest Bayesian
698 Information Criterion (BIC) value. To minimize overfitting, we first determined the optimal
699 number of principal components (PCs) using cross-validation and then ran DAPC
700 retaining the optimal number of PCs and using the identified optimal number of genetic
701 clusters as K to predict group assignment for each sample without *a priori* population

702 information. Ten principal components (PCs) were retained to explain approximately 52%
703 of the total retained variation without our dataset.

704 We also used STRUCTURE v2.3.4 ((Pritchard 2000)) within the program
705 *Structure_threadder* ((Pina-Martins et al. 2017)) to estimate the value of K. We ran
706 STRUCTURE with the admixture model and no prior population information, with an
707 optimal burn-in of 10^4 steps and 10^4 additional steps, and for values of K from 1 to 8 with
708 10 replicates per iteration of K. We used the R package pophelper ((Francis 2017)) to
709 align runs, plot output, and determine the most likely value of K via both ΔK ((Evanno et
710 al. 2005)) and mean probability (MeanLnP(K)). STRUCTURE is known to be sensitive to
711 differences in sample size in populations ((Puechmaille 2016)), which was a factor in our
712 dataset. To eliminate the potential effects of sampling bias on our results, we also ran
713 STRUCTURE using the same conditions for a random subset of $n = 5\text{--}6$ individuals per
714 population, omitting the Russian and Italian samples from the dataset, for values of K
715 from 1 to 5.

716
717

718 **Competing interests**

719 The authors have no competing interests.

720
721

722 **Acknowledgment**

723 This work was supported by the LOEWE-Centre for Translational Biodiversity Genomics
724 (TBG) funded by the Hessen State Ministry of Higher Education, Research and the Arts
725 (HMWK). Funding was also provided by the German Federal Agency for Nature
726 Conservation (BfN) with resources from the Federal Ministry for the Environment, Nature
727 Conservation, Nuclear Safety and Consumer Protection (BMUV), as part of a German-
728 wide project led by the Bund für Umwelt und Naturschutz BUND (Friends of the Earth
729 Germany), Justus Liebig University Gießen, and the Senckenberg Gesellschaft für
730 Naturforschung in the Federal Programme for Biological Diversity called 'In Search of the
731 Garden Dormouse'.

732 We are very grateful to many people who have helped with sample collection: Peter
733 Adamik, Hermann Ansorge, Jonas Astrin, Simon Capt, Stefanie Jessolat, Jeroen van der
734 Kooij, Ines Leonhard, Gernot Segelbacher, David Stille, Adria Viñals Domingo, Frank
735 Zachos, Alain Frantz, Olga Grigoryeva, Maurice La Haye, Roel Baets, Kasper Van Acker,
736 Caren Raditz, Lutz Nielen, Stefanie Erhardt, Jürg Paul Müller, Andrea Krug, Danilo
737 Hartung, Christine Thiel-Bender, Ferry Böhme, Julia Hofmann, Sarah Beer, Jörg und Elli
738 Hacker, Otfried Wüstemann, Sonja Klein, Thomas Doebel, Martina Klotz, Hartmut
739 Schmitt, the Schwarzwald national park, the Museo di Scienze Naturali dell'Alto Adige

740 and Museo di Storia Naturale La Specola di Firenze, Antoni Arrizabalaga, Natural
741 Sciences Museum of Granollers, as well as numerous students and citizen scientists
742 without whom this work would have not been possible. We thank Sarah Stubbe at JLU
743 Gießen for sample preparation.

744

745

746

747 **Data and Code Availability**

748 Genomic and transcriptomics read data and our annotated genome is in the process of
749 being uploaded to NCBI. The haplotype assemblies, gene and transposable element
750 annotations are available for download at
751 <http://genome.senckenberg.de/download/GardenDormouse/>. TOGA annotations are
752 available at <https://genome.senckenberg.de/download/TOGA/>. We also provide a
753 genome browser showing our genomes and all annotations at
754 <https://genome.senckenberg.de/>.

755 Most of our analyses relied on publicly available tools and methods. New scripts are
756 available at https://github.com/pabyerly/TBG_GardenDormouse.

757

758

759 **References**

760 Anděra M. 1986. Dormice (Gliridae) in Czechoslovakia. Part I. : *Glis glis*, *Eliomys quercinus*
761 (Rodentia: Mammalia). *Folia Musei Rerum Naturalium Bohemiae Occidentalis, Plzeň - Zoologica* **24**:
762 3–47.

763 Arvidsson S, Fartmann B, Winkler S, Zimmermann W. 2016. Technical note: Efficient high-
764 throughput SNP discovery and genotyping using normalised genotyping by sequencing (nGBS).
765 [https://biosearch-cdn.azureedge.net/assetsv6/efficient-high-throughput-snp-discovery-genotyping-
766 ngbs-app-note.pdf](https://biosearch-cdn.azureedge.net/assetsv6/efficient-high-throughput-snp-discovery-genotyping-ngbns-app-note.pdf) (Accessed January 6, 2024).

767 Astashyn A, Tvedte ES, Sweeney D, Sapojnikov V, Bouk N, Joukov V, Mozes E, Strope PK, Sylla
768 PM, Wagner L, et al. 2023. Rapid and sensitive detection of genome contamination at scale with
769 FCS-GX. *bioRxiv*. <http://dx.doi.org/10.1101/2023.06.02.543519>.

770 Bennett D, Richard FJ. 2021. Distribution modelling of the garden dormouse *Eliomys quercinus*
771 (Linnaeus, 1766) with novel climate change indicators. *Mamm Biol* **101**: 589–599.

772 Bertolino S. 2017. Distribution and status of the declining garden dormouse *Eliomys quercinus*.
773 *Mammal Review* **47**: 133–147. <http://dx.doi.org/10.1111/mam.12087>.

774 Bertolino S, Colangelo P, Mori E, Capizzi D. 2015. Good for management, not for conservation: an
775 overview of research, conservation and management of Italian small mammals. *Hystrix*.
776 http://www.italian-journal-of-mammalogy.it/pdf-77188-13341?filename=Good%20for%20management_not.pdf.

778 Bertolino S, Viano C, Currado I. 2001. Population dynamics, breeding patterns and spatial use of

779 the garden dormouse (*Eliomys quercinus*) in an Alpine habitat. *J Zool* **253**: 513–521.

780 Blumer M, Brown T, Freitas MB, Destro AL, Oliveira JA, Morales AE, Schell T, Greve C, Pippel M,
781 Jebb D, et al. 2022. Gene losses in the common vampire bat illuminate molecular adaptations to
782 blood feeding. *Sci Adv* **8**: eabm6494.

783 Böhne A, Thiel-Bender C, Kukowka S, Darwin Tree of Life Barcoding collective, Wellcome Sanger
784 Institute Tree of Life programme, Wellcome Sanger Institute Scientific Operations: DNA Pipelines
785 collective, Tree of Life Core Informatics collective, Darwin Tree of Life Consortium. 2023. The
786 genome sequence of the hazel dormouse, *Muscardinus avellanarius* (Linnaeus, 1758). *Wellcome
787 Open Research* **8**. <https://wellcomeopenresearch.org/articles/8-514> (Accessed January 30, 2024).

788 Brandies P, Peel E, Hogg CJ, Belov K. 2019. The Value of Reference Genomes in the Conservation
789 of Threatened Species. *Genes* **10**. <https://pubmed.ncbi.nlm.nih.gov/31717707/>.

790 Burri R, Nater A, Kawakami T, Mugal CF, Olason PI, Smeds L, Suh A, Dutoit L, Bureš S,
791 Garamszegi LZ, et al. 2015. Linked selection and recombination rate variation drive the evolution of
792 the genomic landscape of differentiation across the speciation continuum of Ficedula flycatchers.
793 *Genome Res* **25**: 1656–1665.

794 Campana MG, Parker LD, Hawkins MTR, Young HS, Helgen KM, Szykman Gunther M, Woodroffe
795 R, Maldonado JE, Fleischer RC. 2016. Genome sequence, population history, and pelage genetics
796 of the endangered African wild dog (*Lycaon pictus*). *BMC Genomics* **17**: 1013.

797 Cheng H, Concepcion GT, Feng X, Zhang H, Li H. 2021. Haplotype-resolved de novo assembly
798 using phased assembly graphs with hifiasm. *Nat Methods* **18**: 170–175.

799 Chen S. 2023. Ultrafast one-pass FASTQ data preprocessing, quality control, and deduplication
800 using fastp. *Imeta* **2**. <https://onlinelibrary.wiley.com/doi/10.1002/imt2.107>.

801 Chen S, Zhou Y, Chen Y, Gu J. 2018. fastp: an ultra-fast all-in-one FASTQ preprocessor.
802 *Bioinformatics* **34**: i884–i890.

803 Combe FJ, Juškaitis R, Trout RC, Bird S, Ellis JS, Norrey J, Al-Fulaij N, White I, Harris WE. 2023.
804 Density and climate effects on age-specific survival and population growth: consequences for
805 hibernating mammals. *Anim Conserv* **26**: 317–330.

806 Danecek P, Auton A, Abecasis G, Albers CA, Banks E, DePristo MA, Handsaker RE, Lunter G,
807 Marth GT, Sherry ST, et al. 2011. The variant call format and VCFtools. *Bioinformatics* **27**: 2156–
808 2158.

809 Danecek P, Bonfield JK, Liddle J, Marshall J, Ohan V, Pollard MO, Whitwham A, Keane T,
810 McCarthy SA, Davies RM, et al. 2021. Twelve years of SAMtools and BCFtools. *Gigascience* **10**:
811 giab008.

812 DeSaix MG, Bulluck LP, Eckert AJ, Viverette CB, Boves TJ, Reese JA, Tonra CM, Dyer RJ. 2019.
813 Population assignment reveals low migratory connectivity in a weakly structured songbird. *Mol Ecol*
814 **28**: 2122–2135.

815 du Plessis SJ, Blaxter M, Koepfli K-P, Chadwick EA, Hailer F. 2023. Genomics reveals complex
816 population history and unexpected diversity of Eurasian otters (*Lutra lutra*) in Britain relative to
817 genetic methods. *Mol Biol Evol* **40**. <https://dx.doi.org/10.1093/molbev/msad207>.

818 Evanno G, Regnaut S, Goudet J. 2005. Detecting the number of clusters of individuals using the
819 software STRUCTURE: A simulation study. *Mol Ecol* **14**: 2611–2620.

820 Formenti G, Theissinger K, Fernandes C, Bista I, Bombarely A, Bleidorn C, Ciofi C, Crottini A,
821 Godoy JA, Höglund J, et al. 2022. The era of reference genomes in conservation genomics. *Trends*
822 in *Ecology and Evolution* **37**: 197–202. <https://www.>

823 Francis RM. 2017. pophelper: an R package and web app to analyse and visualize population
824 structure. *Mol Ecol Resour* **17**: 27–32.

825 Frankish A, Diekhans M, Jungreis I, Lagarde J, Loveland JE, Mudge JM, Sisu C, Wright JC,
826 Armstrong J, Barnes I, et al. 2021. GENCODE 2021. *Nucleic Acids Res* **49**: D916–D923.

827 Gautier M, Moazami-Goudarzi K, Levéziel H, Parinello H, Grohs C, Rialle S, Kowalczyk R, Flori L.
828 2016. Deciphering the Wisent Demographic and Adaptive Histories from Individual Whole-Genome
829 Sequences. *Mol Biol Evol* **33**: 2801–2814.

830 Gippoliti S, Amori G. 2007. Beyond threatened species and reintroduction: establishing priorities for
831 conservation and breeding programmes for European rodents in zoos. *International Zoo Yearbook*
832 **41**: 194–202.

833 Giroud S, Ragger MT, Baille A, Hoelzl F, Smith S, Nowack J, Ruf T. 2023. Food availability
834 positively affects the survival and somatic maintenance of hibernating garden dormice (*Eliomys*
835 *quercinus*). *Front Zool* **20**: 1–11.

836 Goudet AJ, Goudet MJ. 2014. Package “ hierfstat .”

837 Halley DJ, Saveljev AP, Rosell F. 2021. Population and distribution of beavers *Castor fiber* and
838 *Castor canadensis* in Eurasia. *Mamm Rev* **51**: 1–24.

839 Harris RS. 2007. Improved pairwise alignment of genomic DNA. The Pennsylvania State University,
840 Ann Arbor, United States <https://www.proquest.com/dissertations-theses/improved-pairwise-alignment-genomic-dna/docview/304835295/se-2>.

841

842 Howe K, Chow W, Collins J, Pelan S, Pointon D-L, Sims Y, Torrance J, Tracey A, Wood J. 2021.
843 Significantly improving the quality of genome assemblies through curation. *Gigascience* **10**.
844 <http://dx.doi.org/10.1093/gigascience/giaa153>.

845 Huang N, Li H. 2023. compleasm: a faster and more accurate reimplementation of BUSCO.
846 *Bioinformatics* **39**. <http://dx.doi.org/10.1093/bioinformatics/btad595>.

847 Jombart T, Bateman A. 2008. adegenet: a R package for the multivariate analysis of genetic
848 markers. *Bioinformatics* **24**: 1403–1405.

849 Kennerley RJ, Lacher TE, Hudson MA, Long B, McCay SD, Roach NS, Turvey ST, Young RP.
850 2021. Global patterns of extinction risk and conservation needs for Rodentia and Eulipotyphla.
851 *Diversity and Distributions* **27**: 1792–1806.

852 Kent WJ, Baertsch R, Hinrichs A, Miller W, Haussler D. 2003. Evolution’s cauldron: duplication,
853 deletion, and rearrangement in the mouse and human genomes. *Proc Natl Acad Sci U S A* **100**:
854 11484–11489.

855 Kim D, Paggi JM, Park C, Bennett C, Salzberg SL. 2019. Graph-based genome alignment and
856 genotyping with HISAT2 and HISAT-genotype. *Nat Biotechnol* **37**: 907–915.

857 Kirilenko BM, Munegowda C, Osipova E, Jebb D, Sharma V, Blumer M, Morales AE, Ahmed A-W,
858 Kontopoulos D-G, Hilgers L, et al. 2023. Integrating gene annotation with orthology inference at
859 scale. *Science* **380**: eabn3107.

860 Lane JE, Kruuk LEB, Charmantier A, Murie JO, Dobson FS. 2012. Delayed phenology and reduced
861 fitness associated with climate change in a wild hibernator. *Nature* **489**: 554–557.

862 Lang J, Büchner S, Meinig H, Bertolino S. 2022. Do We Look for the Right Ones? An Overview of
863 Research Priorities and Conservation Status of Dormice (Gliridae) in Central Europe. *Sustainability*
864 (*Switzerland*) **14**: 9327. <https://www.mdpi.com/2071-1050/14/15/9327/htm>.

865 Leyhausen J, Cocchiararo B, Nowak C, Ansorge H, Bertolino S, Büchner S, Fietz J, Foppen R,
866 Juškaitis R, La Haye M, et al. 2022. Genotyping-by-sequencing based SNP discovery in a non-
867 model rodent, the endangered hazel dormouse. *Conserv Genet Resour* **14**: 195–201.

868 Libois R, Ramalhinho MG, Rosoux R. 2012. Evidence for a differentiated chromosomal race north of
869 classical south European refuge areas in the garden dormouse *Eliomys quercinus*. *Acta Theriol* **57**:
870 313–320.

871 Li H. 2013. Aligning sequence reads, clone sequences and assembly contigs with BWA-MEM. *arXiv*
872 [*q-bioGN*]. <http://arxiv.org/abs/1303.3997>.

873 Li H. 2011. A statistical framework for SNP calling, mutation discovery, association mapping and
874 population genetical parameter estimation from sequencing data. *Bioinformatics* **27**: 2987–2993.

875 Li H. 2018. Minimap2: pairwise alignment for nucleotide sequences. *Bioinformatics* **34**: 3094–3100.

876 Li H, Durbin R. 2011. Inference of human population history from individual whole-genome
877 sequences. *Nature* **475**: 493–496.

878 Luo H, Jiang X, Li B, Wu J, Shen J, Xu Z, Zhou X, Hou M, Huang Z, Ou X, et al. 2023. A high-quality
879 genome assembly highlights the evolutionary history of the great bustard (*Otis tarda*, Otidiformes).
880 *Communications Biology* **6**: 1–11.

881 Lu X, Costeur L, Hugueney M, Maridet O. 2021. New data on early Oligocene dormice (Rodentia,
882 Gliridae) from southern Europe: phylogeny and diversification of the family. *J Syst Palaeontol* **19**:
883 169–189.

884 Mahlert B, Gerritsmann H, Stalder G, Ruf T, Zahariev A, Blanc S, Giroud S. 2018. Implications of
885 being born late in the active season for growth, fattening, torpor use, winter survival and fecundity.
886 *Elife* **7**. <http://dx.doi.org/10.7554/elife.31225>.

887 Malomane DK, Reimer C, Weigend S, Weigend A, Sharifi AR, Simianer H. 2018. Efficiency of
888 different strategies to mitigate ascertainment bias when using SNP panels in diversity studies. *BMC*
889 *Genomics* **19**: 22.

890 Manichaikul A, Mychaleckyj JC, Rich SS, Daly K, Sale M, Chen WM. 2010. Robust relationship
891 inference in genome-wide association studies. *Bioinformatics* **26**: 2867–2873.

892 Martchenko D, Shafer ABA. 2023. Contrasting whole-genome and reduced representation
893 sequencing for population demographic and adaptive inference: an alpine mammal case study.
894 *Heredity* **131**: 273–281.

895 Mead D, Fingland K, Cripps R, Portela Miguez R, Smith M, Corton C, Oliver K, Skelton J, Betteridge
896 E, Doucet J, et al. 2020. The genome sequence of the eastern grey squirrel, *Sciurus carolinensis*
897 Gmelin, 1788. *Wellcome Open Res* **5**: 27.

898 Meinig H, Büchner S. 2012. The current situation of the garden dormouse (*Eliomys quercinus*) in
899 Germany. *Peckiana* **8**: 129–134.

900 Meinig H, Büchner S, Lang J, von Thaden A, Reiners TE, Nowak C, Nava TF, Parcsettich EM,
901 Brünner H, Andersen A, et al. 2023. „Spurensuche Gartenschläfer“—ein Citizen-Science-Projekt zum
902 Schutz einer gefährdeten Schläfmaus in Deutschland ” In search of the garden dormouse ” - A
903 citizen science project to protect an endangered dormouse species in Germany. *Natur und*
904 *Landschaft* **8**: 382–390.

905 Milholland B, Dong X, Zhang L, Hao X, Suh Y, Vijg J. 2017. Differences between germline and
906 somatic mutation rates in humans and mice. *Nat Commun* **8**: 15183.

907 Moritz C. 1994. Defining “ Evolutionarily Significant Units ” for conservation. *Trees* **9**: 373–375.

908 Mouton A, Mortelliti A, Grill A, Sara M, Kryštufek B, Juškaitis R, Latinne A, Amori G, Randi E,
909 Büchner S, et al. 2017. Evolutionary history and species delimitations: a case study of the hazel
910 dormouse, *Muscardinus avellanarius*. *Conserv Genet* **18**: 181–196.

911 Nadachowski A, Daoud A. 1995. Patterns of myoxid evolution in the Pliocene and Pleistocene of
912 Europe. *Hystrix-italian Journal of Mammalogy* **6**.
913 https://doc.rero.ch/record/15906/files/PAL_E3309.pdf (Accessed February 14, 2024).

914 Nieto-Blázquez ME, Schreiber D, Mueller SA, Koch K, Nowak C, Pfenninger M. 2022. Human
915 impact on the recent population history of the elusive European wildcat inferred from whole genome
916 data. *BMC Genomics* **23**: 1–14.

917 O’Connell KA, Mulder KP, Maldonado J, Currie KL, Ferraro DM. 2019. Sampling related individuals
918 within ponds biases estimates of population structure in a pond-breeding amphibian. *Ecol Evol* **9**:
919 3620–3636.

920 Osipova E, Hecker N, Hiller M. 2019. RepeatFiller newly identifies megabases of aligning repetitive
921 sequences and improves annotations of conserved non-exonic elements. *Gigascience* **8**.
922 <http://dx.doi.org/10.1093/gigascience/giz132>.

923 Paez S, Kraus RHS, Shapiro B, Gilbert MTP, Jarvis ED. 2022. Reference genomes for
924 conservation. *Science* **377**: 364–366.

925 Pérez-España S. 2017. Conservation genetics in the European Union – Biases, gaps and future
926 directions. *Biol Conserv* **209**: 130–136.

927 Perez GCL, Libois R, Nieberding CM. 2013. Phylogeography of the garden dormouse *Eliomys*
928 *quercinus* in the western Palearctic region. *J Mammal* **94**: 202–217.

929 Peterson BK, Weber JN, Kay EH, Fisher HS, Hoekstra HE. 2012. Double digest RADseq: An
930 inexpensive method for de novo SNP discovery and genotyping in model and non-model species.
931 *PLoS One* **7**. <http://dx.doi.org/10.1371/journal.pone.0037135>.

932 Pina-Martins F, Silva DN, Fino J, Paulo OS. 2017. Structure_threader: An improved method for
933 automation and parallelization of programs structure, fastStructure and Maverick on multicore CPU
934 systems. *Mol Ecol Resour* **17**: e268–e274.

935 Poplin R, Chang P-C, Alexander D, Schwartz S, Colthurst T, Ku A, Newburger D, Dijamco J,
936 Nguyen N, Afshar PT, et al. 2018. A universal SNP and small-indel variant caller using deep neural
937 networks. *Nat Biotechnol* **36**: 983–987.

938 Pritchard JK. 2000. Inference of population structure using multi-locus genotypes. *Genetics* **155**:
939 945–959.

940 Puechmaille SJ. 2016. The program structure does not reliably recover the correct population
941 structure when sampling is uneven: Subsampling and new estimators alleviate the problem. *Mol*
942 *Ecol Resour* **16**: 608–627.

943 Rammou D-L, Astaras C, Migli D, Boutsis G, Galanaki A, Kominos T, Youlatos D. 2022. European
944 ground squirrels at the edge: Current distribution status and anticipated impact of climate on
945 Europe's southernmost population. *Land (Basel)* **11**: 301.

946 Reiners TE, Eidenschenk J, Neumann K, Nowak C. 2014. Preservation of genetic diversity in a wild
947 and captive population of a rapidly declining mammal, the Common hamster of the French Alsace
948 region. *Mamm Biol* **79**: 240–246.

949 Rhee A, McCarthy SA, Fedrigo O, Damas J, Formenti G, Koren S, Uliano-Silva M, Chow W,
950 Fungtammasan A, Kim J, et al. 2021. Towards complete and error-free genome assemblies of all
951 vertebrate species. *Nature* **592**: 737–746.

952 Rhee A, Walenz BP, Koren S, Phillippy AM. 2020. Merqury: reference-free quality, completeness,
953 and phasing assessment for genome assemblies. *Genome Biol* **21**: 245.

954 Rochette NC, Rivera-Colón AG, Catchen JM. 2019. Stacks 2: Analytical methods for paired-end
955 sequencing improve RADseq-based population genomics. *Mol Ecol* **28**: 4737–4754.

956 Sambrook J, Russell WD. Protocol: DNA isolation from mammalian tissue. *Molecular Cloning: A*
957 *Laboratory Manual (Sambrook J.*

958 Schaub M, Vaterlaus-Schlegel C. 2001. Annual and seasonal variation of survival rates in the
959 garden dormouse (*Eliomys quercinus*). *J Zool* **255**: 89–96.

960 Severn-Ellis AA, Scheben A, Neik TX, Saad NSM, Pradhan A, Batley J. 2020. Genotyping for
961 species identification and diversity assessment using double-digest restriction site-associated DNA
962 sequencing (ddRAD-Seq). In *Methods in Molecular Biology*, Vol. 2107 of, pp. 159–187, Humana
963 Press Inc.

964 Sharma V, Hiller M. 2017. Increased alignment sensitivity improves the usage of genome
965 alignments for comparative gene annotation. *Nucleic Acids Res* **45**: 8369–8377.

966 Shumate A, Wong B, Pertea G, Pertea M. 2022. Improved transcriptome assembly using a hybrid of
967 long and short reads with StringTie. *PLoS Comput Biol* **18**: e1009730.

968 Stamatakis A. 2014. RAxML version 8: a tool for phylogenetic analysis and post-analysis of large
969 phylogenies. *Bioinformatics* **30**: 1312–1313.

970 Suarez HG, Langer BE, Ladde P, Hiller M. 2017. chainCleaner improves genome alignment
971 specificity and sensitivity. *Bioinformatics* **33**: 1596–1603.

972 Szarmach SJ, Brelsford A, Witt CC, Toews DPL. 2021. Comparing divergence landscapes from
973 reduced-representation and whole genome resequencing in the yellow-rumped warbler (*Setophaga*
974 *coronata*) species complex. *Mol Ecol* **30**: 5994–6005.

975 Takach BV, Sargent H, Penton CE, Rick K, Murphy BP, Neave G. 2023. Population genomics and
976 conservation management of the threatened black-footed tree-rat (*Mesembriomys gouldii*) in
977 northern Australia. 1–11.

978 Talla V, Mrazek V, Höglund J, Backström N. 2023. Whole genome re-sequencing uncovers
979 significant population structure and low genetic diversity in the endangered clouded apollo

980 (Parnassius mnemosyne) in Sweden. *Conserv Genet*. <https://doi.org/10.1007/s10592-023-01502-9>.

982 Theissinger K, Fernandes C, Formenti G, Bista I, Berg PR, Bleidorn C, Bombarely A, Crottini A,
983 Gallo GR, Godoy JA, et al. 2023. How genomics can help biodiversity conservation. *Trends in*
984 *Genetics* **39**: 545–559. <https://doi.org/10.1016/j.tig.2023.01.005>.

985 Tsuchiya MTN, Dikow RB, Cassin-Sackett L. 2020. First Genome Sequence of the Gunnison's
986 Prairie Dog (*Cynomys gunnisoni*), a Keystone Species and Player in the Transmission of Sylvatic
987 Plague. *Genome Biol Evol* **12**: 618–625.

988 Uchimura A, Higuchi M, Minakuchi Y, Ohno M, Toyoda A, Fujiyama A, Miura I, Wakana S, Nishino
989 J, Yagi T. 2015. Germline mutation rates and the long-term phenotypic effects of mutation
990 accumulation in wild-type laboratory mice and mutator mice. *Genome Res* **25**: 1125–1134.

991 Verde Arregoitia LD. 2016. Biases, gaps, and opportunities in mammalian extinction risk research.
992 *Mamm Rev* **46**: 17–29.

993 Viluma A, Flagstad Ø, Åkesson M, Wikenros C, Sand H, Wabakken P, Ellegren H. 2022. Whole-
994 genome resequencing of temporally stratified samples reveals substantial loss of haplotype diversity
995 in the highly inbred Scandinavian Wolf population. *Genome Res* **32**: 449–458.

996 Wang J. 2018. Effects of sampling close relatives on some elementary population genetics
997 analyses. *Mol Ecol Resour* **18**: 41–54.

998 Weir BS, Cockerham CC. 1984. Estimating F-Statistics for the Analysis of Population Structure.
999 *Evolution* **38**: 1358.

1000 Wolf JF, Bowman J, Keobouasone S, Taylor RS, Wilson PJ. 2022. A de novo genome assembly
1001 and annotation of the southern flying squirrel (*Glaucomys volans*). *G3* **12**.
1002 <http://dx.doi.org/10.1093/g3journal/jkab373>.

1003 Wright BR, Farquharson KA, McLennan EA, Belov K, Hogg CJ, Gruuber CE. 2020. A demonstration
1004 of conservation genomics for threatened species management. *Mol Ecol Resour* **20**: 1526–1541.

1005 Yu G, Smith DK, Zhu H, Guan Y, Lam TTY. 2017. ggtree: an r package for visualization and
1006 annotation of phylogenetic trees with their covariates and other associated data. *Methods Ecol Evol*
1007 **8**: 28–36.

1008 Zhang H, Song L, Wang X, Cheng H, Wang C, Meyer CA, Liu T, Tang M, Aluru S, Yue F, et al.
1009 2021. Fast alignment and preprocessing of chromatin profiles with Chromap. *Nat Commun* **12**:
1010 6566.

1011 Zheng X, Levine D, Shen J, Gogarten SM, Laurie C, Weir BS. 2012. A high-performance computing
1012 toolset for relatedness and principal component analysis of SNP data. *Bioinformatics* **28**: 3326–
1013 3328.

1014 Zhou C, McCarthy SA, Durbin R. 2023. YaHS: yet another Hi-C scaffolding tool. *Bioinformatics* **39**.
1015 <http://dx.doi.org/10.1093/bioinformatics/btac808>.

1016 Zoonomia Consortium. 2020. A comparative genomics multitool for scientific discovery and
1017 conservation. *Nature* **587**: 240–245.